

# Counterion Adsorption on Flexible Polyelectrolytes: Comparison of Theories

Rajeev Kumar, Arindam Kundagrami, and M. Muthukumar\*

Department of Polymer Science & Engineering, Materials Research Science & Engineering Center, University of Massachusetts, Amherst, Massachusetts 01003

Received August 6, 2008; Revised Manuscript Received December 16, 2008

**ABSTRACT:** Counterion adsorption on a flexible polyelectrolyte chain in a spherical cavity is considered by taking a “permuted” charge distribution on the chain so that the “adsorbed” counterions are allowed to move along the backbone. We compute the degree of ionization by using self-consistent field theory (SCFT) and compare it with the previously developed variational theory. An analysis of various contributions to the free energy in both theories reveals that the equilibrium degree of ionization is attained mainly as an interplay of the adsorption energy of counterions on the backbone, the translational entropy of the small ions, and their correlated density fluctuations. The degree of ionization computed from SCFT is significantly lower than that from the variational formalism. The difference is entirely due to the density fluctuations of the small ions in the system, which are accounted for in the variational procedure. When these fluctuations are deliberately suppressed in the truncated variational procedure, there emerges a remarkable quantitative agreement in the various contributing factors to the equilibrium degree of ionization despite the fundamental differences in the approximations and computational procedures used in these two schemes. Furthermore, it is found that the total free energies from the truncated variational procedure and the SCFT are in quantitative agreement at low monomer densities and differ from each other at higher monomer densities. The disagreement at higher monomer densities is due to the inability of the variational calculation to compute the solvent entropy accurately at higher concentrations. A comparison of electrostatic energies (which are relatively small) reveals that the Debye–Hückel estimate used in the variational theory is an overestimation of electrostatic energy as compared with the Poisson–Boltzmann estimate. Nevertheless, because the significant effects from density fluctuations of small ions are not captured by the SCFT and because of the close agreement between SCFT and the other contributing factors in the more transparent variational procedure, the latter is a better computational tool for obtaining the degree of ionization.

## I. Introduction

Counterion adsorption in polyelectrolyte solutions is one of the fundamental problems in polyelectrolyte physics, which has been a topic of extensive research<sup>1–28</sup> for decades. Historically,<sup>1–4</sup> the counterion adsorption in polyelectrolyte solutions was described as an analog of ion-pairing in simple electrolyte solutions, and deviations from the Debye–Hückel limiting laws in colligative properties of polyelectrolyte solutions in dilute concentration regime had been attributed to counterion adsorption. By ignoring interactions among different chains in dilute solutions, modeling a polyelectrolyte chain by an infinite rod, and using bulk dielectric constant of the medium to describe electrostatic interactions, counterion adsorption (or Manning condensation) was predicted to be a result of a singularity in the partition function arising because of a singular electrostatic potential near the rod. In particular, it was predicted that for monovalent monomers and counterions, if  $l_B/b > 1$ , where  $l_B$  is Bjerrum length ( $= e^2/4\pi\epsilon_0\epsilon k_B T$ , with  $e$  being the electronic charge,  $\epsilon_0$  being the dielectric constant of the vacuum,  $\epsilon$  being the dielectric constant of the medium, and  $k_B T$  being the Boltzmann constant times temperature) and  $b$  is the charge spacing on the backbone of the chain, then some of the counterions from the solution adsorb on the chain until  $l_B/b = 1$ . However, if  $l_B/b < 1$ , then the Debye–Hückel approximation (i.e., the linearization of Poisson–Boltzmann) can be used to describe the electrostatics, and there is no adsorption. In other words, counterion adsorption was described as a kind of phase transition (such as the condensation of vapors) driven by only electrostatic energy.

Over the years, simulations<sup>5–12</sup> and experiments<sup>13–19</sup> have provided insight into the counterion adsorption mechanism in polyelectrolyte solutions. Most importantly, it was revealed that a polyelectrolyte chain never attains a perfect rod conformation, even in salt-free solutions where the rod conformation is usually expected. Also, it has been shown that the effect of ion pairing<sup>6,17</sup> on the backbone and dielectric constant<sup>18</sup> has to be considered to treat a realistic polyelectrolyte chain. Furthermore, simulations<sup>7,8</sup> reveal that the counterions retain their translational degrees of freedom along the backbone of the chain after being adsorbed.

These insights obtained from the simulations and experiments have led to a number of theoretical descriptions<sup>20–28</sup> of the counterion adsorption in polyelectrolyte solutions (containing monovalent or multivalent salts) over the last two decades. For an isolated, single polyelectrolyte chain, it was shown that there is no singularity in the partition function when the polyelectrolyte chain is modeled as a flexible one.<sup>26</sup> An important prediction of the theory<sup>26</sup> emphasized the role played by the dielectric mismatch between the local environment of the backbone and the bulk solution in driving counterion adsorption, and that had not been previously highlighted in the literature. In particular, it was shown that counterion adsorption arises as an interplay of adsorption energy and translational entropy of ions. Entropically, a higher degree of ionization, an effect that is opposed by the lowering of electrostatic energy by the formation of ion pairs at the backbone of the chain, is preferred. To carry out the calculations analytically, the Debye–Hückel potential was used to describe the electrostatic interactions between charged species, and a novel variational method was used to express the chain conformational entropy and excluded volume effects. Finally, the complete free energy of the system (consisting of the chain, the counterions, and the solvent) was

\*To whom correspondence should be addressed. E-mail: muthu@polysci.umass.edu.

**Table 1. Comparison of Contributions to  $F_i^*$  in SCFT and Variational Formalism**

term	SCFT	variational formalism
$E_w - TS_s$	$\chi_{ps} l^3 \int dr \rho_p(r) \rho_s(r) + \rho_0 \int dr n(r) + f \int dr \rho_s(r) \{\ln[\rho_s(r)] - 1\}$	$4/3 (3/2\pi)^{3/2} (1 - 2\chi_{ps}) \sqrt{N/l^3} + \chi_{ps} N l^3 - \Omega$
$E_c$	$1/2 \int dr \psi(r) \rho_c(r)$	$2\sqrt{6} \int_{\pi}^{\pi/2} \tilde{l}_B N^{3/2} \Theta_0(a)/\tilde{l}_1^{1/2}$
$-TS_i$	$\sum_{j=c,+,-} \int dr \rho_j(r) \{\ln[\rho_j(r)] - 1\}$	$(fN + n_+) \ln[(fN + n_+)/\Omega] + n_- \ln(n_-/\Omega) - (fN + n_+ + n_-)$
$-TS_p$	$-\ln[(\int dr q(r, N))/(\int dr q_0(r, N))] - \rho_0 \int dr n(r) - f \int dr [\{Z_p \Psi(r) + w_p(r)\} \rho_p(r)]$	$3/2 [\tilde{l}_1 - 1 - \ln \tilde{l}_1]$

simultaneously minimized in terms of the degree of counterion adsorption and the size of the polyelectrolyte chain to self-consistently obtain the equilibrium values of the respective variables. The theory is in qualitative agreement with the known simulation results. Recently, this single-chain theory has been extended to describe the competitive counterion adsorption<sup>28</sup> phenomenon in the presence of multivalent and monovalent counterions. Despite the qualitative agreements with simulations and experiments (especially regarding the phenomena of charge reversal and reentrant transition), the approximations used in the theory have not been rigorously assessed so far.

In this work, we consider the counterion adsorption on a flexible polyelectrolyte chain in a spherical cavity in the presence of monovalent salt. Physically, such a situation is realized in extremely dilute polyelectrolyte solutions, where interchain interactions can be safely ignored and a finite volume can be carved out for each chain and in pores confining polyelectrolyte chains, depending on the ratio of the cavity size to the radius of gyration of the polymer. We used the self-consistent field theory (SCFT) to compute the equilibrium degree of counterion adsorption. SCFT computes the free energy of the system by summing over all possible conformations of the chain and hence providing a more accurate description of the system compared with the variational formalism. (In fact, it provides the exact free energy at the mean-field level.) Also, because the electrostatics in SCFT is treated at full, nonlinear Poisson–Boltzmann level, we can assess the validity of the Debye–Hückel potential to describe the electrostatic energy in the variational formalism. Although SCFT provides an accurate and clear picture, it is computationally expensive to calculate the degree of ionization because of a vast parameter space in the case of polyelectrolytes. However, the variational theory put forward by Muthukumar<sup>26</sup> is transparent, analytically tractable (to some extent), and very inexpensive in terms of the computational needs. The aim of this study is to provide a simple, accurate, and easy-to-use method to compute the degree of ionization and assess the approximations used in the variational formalism.

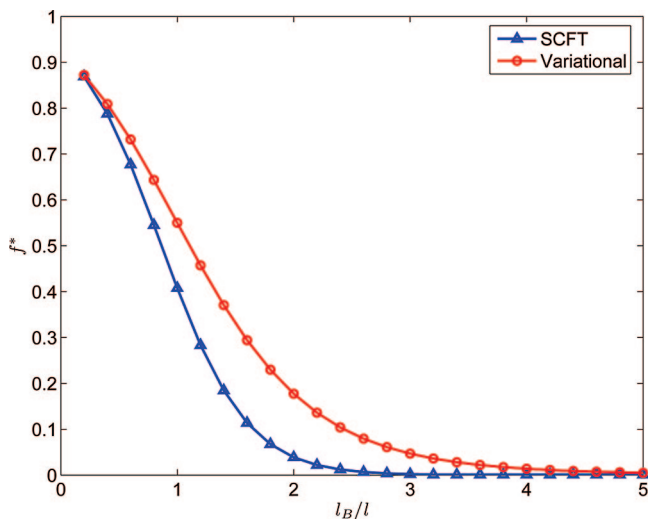


**Figure 1.** Comparison of SCFT and the variational formalism (with one-loop corrections) to illustrate the effect of correlations among small ions on the effective degree of ionization ( $f^*$ ).  $Z_p = -Z_c = -1$ ,  $R/l = 10$ ,  $N = 100$ ,  $c_s = 0.1M$ ,  $\chi_{ps} = 0.45$ , and  $\delta = 3$ .

This Article is organized as follows: the theoretical formalisms are presented in section II, and the calculated results and conclusions are presented in sections III and IV, respectively.

## II. Comparison of Theories: Self-Consistent Field Theory and Variational Formalism

We consider a single flexible polyelectrolyte chain of total  $N$  Kuhn segments, each with length,  $l$ , confined in a spherical cavity of volume  $\Omega = 4\pi R^3/3$ . The polyelectrolyte chain is represented as a continuous curve of length  $Nl$ , and an arc length variable,  $t$ , is used to represent any segment along the backbone so that  $t \in [0, Nl]$ . Now we assume that the chain (negatively charged) is surrounded by  $n_c$  monovalent counterions (positively charged) released by the chain along with  $n_\gamma$  ions of species  $\gamma$  ( $= +, -$ ) coming from added salt so that the whole system is globally electroneutral. Let  $Z_j$  be the valency (with sign) of the charged species of type  $j$  and  $n_s$  be the number of solvent molecules (satisfying the incompressibility constraint after assuming the small ions to be pointlike) present in the cavity. For simplicity, we have taken the volume of a solvent molecule ( $v_s$ ) to be equal to the volume of the monomer (i.e.,  $v_s \equiv l^3$ ). Subscripts p, s, c, +, and  $-$  are used to represent monomer, solvent, counterion from polyelectrolyte, and positive and negative salt ions, respectively.

To study counterion adsorption, we use the so-called two-state model for the counterions so that there are two populations of counterions in the system. One population of the counterions is free to enjoy the available volume (called the free counterions), and the other population is adsorbed on the backbone. However, the adsorbed counterions are allowed to enjoy translational degrees of freedom along the backbone, maintaining a total charge of  $efNZ_p$  on the chain, where  $e$  is the electronic charge and  $f$  is the degree of ionization of the chain (i.e., there are  $-(1 - f)NZ_p/Z_c$  adsorbed counterions on the chain). In the literature, this kind of charge distribution has been referred to as a permuted charge distribution.<sup>29</sup>

For a particular set of parameters, we compute the free energy of the system comprising the single chain, its counterions, the salt ions, and the solvent as a function of the degree of ionization ( $f$ ). As mentioned before, we compute the free energy using two different computational frameworks: SCFT<sup>30,31</sup> and the variational<sup>26,32,33</sup> formalism. In both of the formalisms, we ignore the electrostatic interactions between solvent molecules and the small ions and model the dielectric constant ( $\epsilon$ ) of the medium to be independent of temperature ( $T$ ) to extract energy and entropy of the system. Also, for comparison purposes, we divide the free energy into a mean-field part and an additional part, which goes beyond the mean-field theory. Mean-field part is further divided into the contributions that come from the adsorbed counterions ( $F_a^*$ ) and the free ions and from the chain entropy, and so on ( $F_i^*$ ). All contributions are properly identified (or subdivided into) as the enthalpic and entropic parts. In all of what follows, the superscript  $*$  represents the mean-field part. A brief description of the derivation of the two formalisms is presented in Appendices A and B, and the original references<sup>26,31</sup> may be consulted for details.

To start with, we note that the contributions coming from adsorbed counterions are the same in both formalisms and are given by

$$F_a^* = E_a - TS_a \quad (1)$$

$$E_a = -(1-f)N\delta l_B/l \quad (2)$$

$$-TS_a = N[f \log f + (1-f) \log(1-f)] \quad (3)$$

so that  $E_a$  is the electrostatic binding energy of the ion pairs formed on the polymer backbone because of the adsorption of ions and  $S_a$  is the translational entropy of the adsorbed counterions along the backbone. Parameter  $\delta = \epsilon l / \epsilon_l d$  reflects the deviation of the dielectric constant at the local environment of the chain ( $\epsilon_l$ ) from the bulk value ( $\epsilon$ ), and  $d$  represents the length of the dipole formed because of ion pairing.

**A. Self-Consistent Field Theory.** Although  $F_a^*$  is the same in both formalisms, other contributions that involve the free ions, the chain entropy, and so on (i.e.,  $F_f^*$ ), significantly differ from each other in terms of computational details. In SCFT,  $F_f^*$  is computed after solving for fields experienced by different components in the system, which arise as a result of interactions of a particular component with the others. For a single polyelectrolyte chain in a spherical cavity, each charged component (monomers and small ions) experiences a dimensionless field  $\psi$  (in units of  $k_B T / e$ ), which is given by the solution of the Poisson–Boltzmann equation

$$\nabla_r^2 \psi(r) = -4\pi l_B \rho_e(r) \quad (4)$$

where  $\rho_e(r) = \sum_{j=c,+,-} Z_j \rho_j(r) + Z_p f \rho_p(r)$  is the local charge density and  $\rho_j(r)$  is the collective number density of species of type  $\beta = p, c, +, -$ . Collective number densities for small ions are given by the Boltzmann distribution with the prefactor determined by the constraint that the number of small ions are fixed in the system. Explicitly,

$$\rho_j(r) = \frac{n_j \exp[-Z_j \psi(r)]}{\int dr \exp[-Z_j \psi(r)]} \quad (5)$$

for  $j = c, +, -$ . In eq 4,  $\rho_p(r)$  is the monomer density, which is related to the probability of finding a particular monomer (described by the contour variable,  $t$ ) at a particular location,  $r$ , when the starting end of the chain can be anywhere in space (say,  $q(r, t)$ ) by the relation

$$\rho_p(r) = \frac{\int_0^N dt q(r, t) q(r, N-t)}{\int dr q(r, N)} \quad (6)$$

Furthermore, it can be shown that  $q(r, t)$  satisfies the modified diffusion equation<sup>30,34</sup>

$$\frac{\partial q(r, t)}{\partial t} = \left[ \frac{l^2}{6} \nabla_r^2 - \{Z_p f \psi(r) + w_p(r)\} \right] q(r, t), \quad t \in (0, N) \quad (7)$$

where  $w_p$  is the field experienced by monomers because of nonelectrostatic interactions. At the saddle point, it is given by

$$w_p(r) = \chi_{ps} l^3 \rho_s(r) + \eta(r) \quad (8)$$

where  $\chi_{ps}$  is the dimensionless Flory's chi parameter and  $\eta(r)$  is the Lagrange's multiplier to enforce the incompressibility constraint

$$\rho_p(r) + \rho_s(r) = \rho_0 \quad (9)$$

at all points in the system. Here  $\rho_0$  is the total number density, that is,  $\rho_0 = (N + n_s) / \Omega = 1 / l^3$ . Finally,  $\rho_s(r)$  is the collective number density of solvent molecules given by the Boltzmann distribution in terms of the field experienced by a solvent molecule ( $w_s$ ). Within the saddle-point approximation,  $\rho_s$  and  $w_s$  are related by

$$\rho_s(r) = \frac{n_s \exp[-w_s(r)]}{\int dr \exp[-w_s(r)]} \quad (10)$$

$$w_s(r) = \chi_{ps} l^3 \rho_p(r) + \eta(r) \quad (11)$$

These equations also close the loop of self-consistent equations, and eqs 4–11 form the set of coupled nonlinear equations that defines the system.

After solving these equations for fields (and in turn, for densities), the free energy at the saddle point,  $F_f^*$ , is divided into enthalpic contributions because of the excluded volume and electrostatic interactions and into entropic contributions because of small ions, solvent molecules, and the polyelectrolyte chain. Denoting these contributions by  $E_w$ ,  $E_e$ ,  $S_i$ ,  $S_s$ , and  $S_p$ , respectively,  $F_f^*$  is given by

$$F_f^* - F_0 = E_w + E_e - T(S_i + S_s + S_p) \quad (12)$$

where  $F_0 = (\rho_0) / (2) (N w_{pp} + n_s w_{ss})$  is the self-energy contribution arising from the excluded volume interactions characterized by the excluded volume parameters,  $w_{ij}$ , between species  $i$  and  $j$ . Explicit expressions for different constituents of  $F_f^*$  are presented in Table 1 in terms of densities and fields at the saddle point. Within the saddle-point approximation, the total free energy ( $F_{SCFT}$ ) of the system is given by  $F_{SCFT} \approx F_a^* + F_f^*$ . To compare the free energies obtained from SCFT and the variational formalism for a given  $N$  and  $R$ , a single Gaussian chain of contour length,  $Nl$ , in the volume,  $\Omega$ , is chosen as the reference frame, whose free energy is taken to be zero. This reference free energy of confinement for a single Gaussian chain has been subtracted from the polymer conformational entropy in Table 1. The free energy of confining a single Gaussian chain with  $N$  Kuhn segments of length,  $l$ , each in a spherical cavity of radius,  $R$ , can be computed exactly and is given by<sup>35</sup>

$$F_{\text{gaussian}} = -\ln \left[ \int dr q_0(r, N) \right] \\ = -\ln \left[ \frac{6\Omega}{\pi^2} \sum_{k=1}^{\infty} \frac{1}{k^2} \exp \left[ -\frac{k^2 \pi^2 N l^2}{6R^2} \right] \right] \quad (13)$$

**B. Variational Formalism.** In variational calculations,<sup>26</sup> a single polyelectrolyte chain, whose monomers interact with the excluded volume and the electrostatic interactions in the presence of the small ions, is approximated by an effective Gaussian chain, whose conformational statistics are dependent on the different kinds of interactions in the system. To compute the equilibrium free energy, its variational ansatz is minimized with respect to the variational parameter,  $l_1$ , which is related to the radius of gyration ( $R_g$ ) of the chain by  $R_g^2 = N l_1^2 / 6$ . Physically, this corresponds to the minimization of the free energy of the single-chain system with respect to the size of the chain. For the computations of the equilibrium degree of ionization, an additional minimization of the free energy with respect to the degree of ionization has to be carried out. However, because of the intricate coupling between the size of the chain and the degree of ionization, the minimizations have to be carried out self-consistently.

The variational ansatz of the total free energy ( $F_{\text{variational}}$ ) is given by  $F_{\text{variational}} = F_a^* + F_f^* + \Delta F$ , where  $\Delta F$  involves one-loop fluctuation corrections, addressing the density fluctuations of the small ions, to the free energy. As mentioned before, the free energy of the adsorbed counterions (i.e.,  $F_a^*$ ) is the same in both SCFT and the variational formalisms (cf. eq 1). The  $F_f^*$  part of the free energy<sup>26</sup> is tabulated in Table 1. The function  $\Theta_0(a)$  in Table 1 is a cross-over function given by<sup>26,33</sup>



$$\Theta_0(a) = \frac{\sqrt{\pi}}{2} \left( \frac{2}{a^{5/2}} - \frac{1}{a^{3/2}} \right) \exp(a) \operatorname{erfc}(\sqrt{a}) + \frac{1}{3a} + \frac{2}{a^2} - \frac{\sqrt{\pi}}{2a^{5/2}} - \frac{\sqrt{\pi}}{2a^{3/2}} \quad (14)$$

where  $a \equiv \kappa^2 N l l_i / 6$  and  $\kappa l$  is the dimensionless inverse Debye length. Furthermore,  $\tilde{l}_i = l_i / l$  and  $\tilde{l}_B = l_B / l$ . The number of salt ions ( $n_+$ ,  $n_-$ ) is related to the salt concentration ( $c_s$ ) by the relation  $Z_+ n_+ = -Z_- n_- = 0.6023 c_s \Omega$ , where  $c_s$  is in units of moles per liter (molarity). Also, all of the terms in the free energies are in units of  $k_B T$ .

In this work, we have ignored one-loop corrections to the free energy within SCFT. However, one-loop corrections to the free energy coming from the density fluctuations of the small ions within the variational formalism is given by

$$\Delta F = -\frac{\Omega \kappa^3}{12\pi} \quad (15)$$

where  $\kappa^2 = 4\pi l_B (fN + n_+ + n_-) / \Omega$  and  $\kappa$  is the inverse Debye length.

**C. Numerical Techniques.** We solve SCFT eqs 4–11 within spherical symmetry (i.e.,  $r \rightarrow r = |r|$ ) using the Dirichlet boundary conditions for  $q(r, t)$  and all of the fields except  $\eta(r)$ . Also, because of the use of spherical symmetry in these calculations, we use

$$\left. \frac{\partial \psi(r)}{\partial r} \right|_{r=0} = \left. \frac{\partial q(r, t)}{\partial r} \right|_{r=0} = 0 \text{ for all } t \quad (16)$$

Starting from an initial guess for fields, new fields and densities are computed after solving the modified diffusion and Poisson–Boltzmann equation by finite difference methods.<sup>36</sup> Broyden's method<sup>36</sup> has been used to solve the set of nonlinear equations. The equilibrium value of the degree of ionization ( $f^*$ ) is obtained after minimizing the free energy with respect to  $f$ . We carry out the numerical minimization of free energy over  $f$  by using Brent's method.<sup>36</sup> The results presented in this Article were obtained by using a grid spacing of  $\Delta r = 0.1$  and contour steps of  $\Delta t = 0.01$ .

However, the self-consistent minimization of the free energy in the variational method has been carried out by assuming a uniform expansion of the chain within spherical symmetry. In this formalism, the free energy is simultaneously minimized with respect to  $f$  and  $l_i$ , and both of these quantities at equilibrium ( $f^*$ ,  $l_i^*$ ) are computed self-consistently. The radius of gyration of the chain (which is confined to a finite volume,  $\Omega = 4\pi R^3/3$ ) is obtained from the equilibrium value of the expansion factor,  $l_i^*$ . For these calculations, the upper bound for the radius of gyration of the chain is specified to be the radius of the confining volume (i.e.,  $R_g \leq R$ ) to mimic the confinement effects. Also, the Kuhn step length,  $l$ , is taken to be unity in both variational as well as SCFT calculations.

### III. Results

**A. Degree of Ionization.** We have carried out an exhaustive comparison between the SCFT and variational formalisms by calculating the equilibrium degree of ionization ( $f^*$ ) of a negatively charged single flexible polyelectrolyte chain (i.e.,  $Z_p = -1$ ,  $Z_c = 1$ ) in the presence of a monovalent salt. The equilibrium degree of ionization is determined as a function of the strength of the electrostatic interaction (or Coulomb strength), which is proportional to the Bjerrum length,  $l_B$ , for a given solvent. In both cases, the effective charge expectedly decreases (Figure 1) with higher Coulomb strengths that help a progressively larger degree of adsorption of counterions on the chain backbone. However,  $f^*$  obtained from the variational procedure is systematically higher than that from SCFT. It is

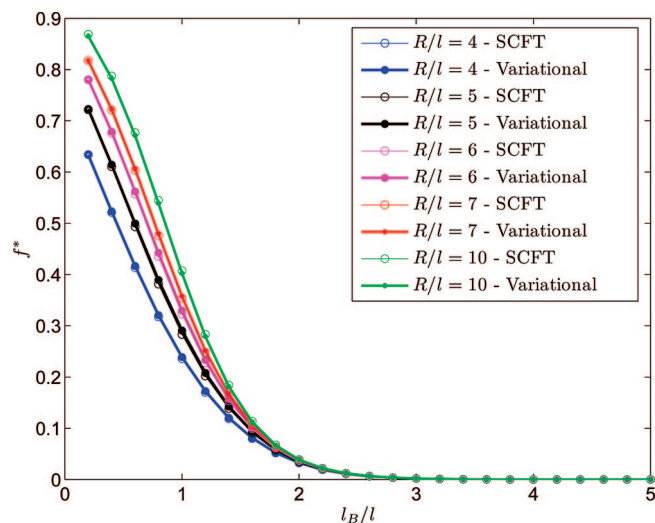


**Figure 2.** Comparison of  $f^*$  computed using SCFT and the variational formalism (without one-loop correction) for different values of  $R$  and  $l_B/l$ .  $Z_p = -Z_c = -1$ ,  $N = 100$ ,  $c_s = 0.1M$ ,  $\chi_{ps} = 0.45$ , and  $\delta = 3$ . Plot for SCFT when  $R/l = 10$  is the same as that in Figure 1.

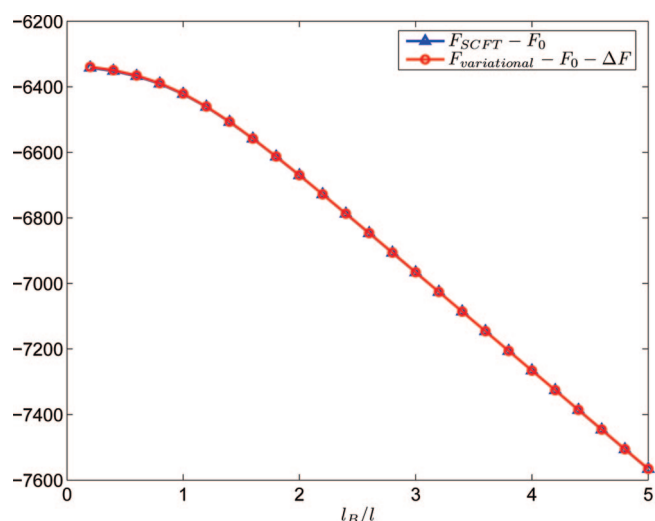


**Figure 3.** Comparison of total free energies (at equilibrium, for  $f = f^*$ ) obtained from SCFT and the variational calculations (without one-loop correction).  $Z_p = -Z_c = -1$ ,  $R/l = 10$ ,  $N = 100$ ,  $c_s = 0.1M$ ,  $\chi_{ps} = 0.45$ , and  $\delta = 3$ .

to be noted that the degree of ionization is essentially zero in SCFT for experimentally relevant values of  $l_B/l$  (around 3 for aqueous solutions), whereas  $f^*$  is reasonable in the variational theory. Although both theories use different approximations and computational procedures, there is one major conceptual input that distinguishes these theories. Whereas the variational formalism of ref 26 includes the density fluctuations of the small ions as one-loop corrections to the free energy, the SCFT does not address these fluctuations. In an effort to quantify the consequences of small ion density fluctuations and then compare the consequences of the rest of the terms in the variational theory against SCFT (which does not contain small ion density fluctuations by construction), we subtract  $\Delta F$  from  $F_{\text{variational}}$  and then compute  $f^*$ . The results are given in Figures 2 and 3.

Remarkably, under different conditions corresponding to widely varying degrees of confinement, the  $f^*$  obtained by the minimization of SCFT free energies is indistinguishable from that obtained using variational free energies without one-loop corrections (i.e.,  $F_{\text{variational}} - \Delta F$ ). We demonstrate this in Figure 2, where we have plotted  $f^*$  as a function of  $l_B/l$  for different

spherical volumes (i.e., different  $R$ ). Therefore, we arrive at two conclusions: (a) density fluctuations of small ions included in the full variational formalism contribute significantly to determining the equilibrium degree of ionization and lead to better values of  $f^*$  than SCFT, and (b) the value of  $f^*$  is remarkably indistinguishable between the SCFT and the variational formalism with deliberate suppression of small ion density fluctuations. The first conclusion can be readily rationalized as follows by considering the two curves in Figure 1.

The increase in  $f^*$  with the inclusion of  $\Delta F$  can be understood by the fact that the density fluctuations of the small ions lower the free energy, and its contribution to the total free energy increases with the increase in the number of free ions (goes like  $-n^{3/2}$  in the salt-free case, where  $n$  is the number of free ions, cf. eq 15). For higher values of  $l_B/l$  (above four), all of the counterions are adsorbed on the chain so that the degree of ionization of the chain is zero irrespective of the density fluctuations. In contrast, for lower values of  $l_B/l$  (below 0.5), the chain is fully ionized, and the effect of the density fluctuations of the small ions on the effective degree of ionization is minimal. However, for the intermediate values of  $l_B/l$ , the density fluctuations of the small ions significantly affect the degree of ionization, and nonmonotonic deviations from the SCFT results as a function of  $l_B/l$  are observed in this regime. Also, a term-by-term comparison of the free-energy components reveals that the discrepancy arises solely because of the term accounting for the density fluctuations of the small ions. This disagreement highlights the fact that the effect of density fluctuations of the small ions is not included in SCFT within the saddle point approximation.

The above second conclusion requires further scrutiny. The remarkable agreement between the two formalisms is surprising because these theories use different approximations and different computational procedures. In the variational formalism of ref 26, which is used in the present Article, the chain swelling due to electrostatic interaction is assumed to be spherically uniform on all length scales and at the level of Debye–Hückel potential between the segments. However, this scheme is more analytically tractable with different contributing factors (Table 1) having explicit physical interpretation. However, in SCFT, the electrostatic interaction is at the nonlinear Poisson–Boltzmann level, and the chain expansion is addressed on all local length scales through fields generated by intersegment potentials. Although the chain conformations are not readily accessible in the standard version of SCFT used here, the free energy of the system can be calculated, and its resolution into entropic and enthalpic parts is possible. In view of such apparently divergent approaches in SCFT and the variational formalisms, we now proceed to make quantitative comparisons between the two in terms of the various contributing factors.

**B. Term-by-Term Comparison of Free Energy: Self-Consistent Field Theory and Variational Formalism.** To assess the approximations used in the variational theory and to find out the origin of the remarkable agreement in terms of the equilibrium effective charge ( $f^*$ ) obtained from SCFT and variational theory (with deliberate suppression of one-loop corrections for small ion density fluctuations), we have compared individual contributions to the free energies in these two formalisms. Before presenting the numerical results, the role of different contributions in driving the counterion adsorption can be qualitatively understood by considering the following physical picture.

The driving forces for the counterion adsorption are the formation of ion pairs due to the presence of strong attractive interactions in the process (self energy of the dipoles) and the decrease in intramolecular electrostatic repulsions (compared with a fully ionized chain, where these repulsions are the

strongest). However, an extensive counterion adsorption on the chain backbone is unfavorable because of the loss in translational degrees of freedom of the free counterions. Another factor that plays a role in this competition of the energy and entropy is the translational entropy of the adsorbed counterions. This entropic feature alone favors a state where half of the charges on the chain backbone are free and the other half adsorb the counterions. With an increase in the electrostatic interaction strength (i.e., Bjerrum length), the driving forces for the counterion adsorption increase and drive more and more counterions to the backbone. However, an extensive counterion adsorption leads to the chain contraction because of lower intramolecular electrostatic repulsions (a result of the lower number of bare charged sites) even when the electrostatic interaction strength is high. However, we show that the counterion adsorption that leads to the lowering of the effective charge (that decreases the electrostatic energy because of the formation of ion pairs) has a bigger effect than the chain contraction (which affects the chain conformational entropy and polymer–solvent entropy) or the increase in intramolecular electrostatic repulsions among the unadsorbed segments as we gradually increase the Bjerrum length. Of course, in addition, correlations of small ion density fluctuations also contribute to  $f^*$  in the full variational calculation. Numerical results on the relative importance of the various contributions to the total free energy along with their role in driving the counterion adsorption are presented below.

To start with, in Figure 3, we have plotted the total free energy calculated in both methods for the following set of parameters:  $Z_p = -Z_c = -1$ ,  $R/l = 10$ ,  $N = 100$ ,  $c_s = 0.1M$ ,  $\delta = 3$ , and  $\chi_{ps} = 0.45$ . It is clear that the total free energies obtained from SCFT and the variational theory are in quantitative agreement with each other.

To analyze this striking agreement between the two methods, we focus on the individual components of the free energy, as tabulated in Table 1. In Figures 4 and 5, we have compared these different constituents of the free energy obtained from both SCFT and the variational formalisms for low monomer densities. It is evident that both theories predict that the major contributions to the free energy are from the ion-pair energy (Figure 4a), the adsorbed counterion translational entropy (Figure 4b), the polymer–solvent interaction energy and the solvent entropy (Figure 4c), and the free ions translational entropy (Figure 4d). Contributions due to the chain conformational entropy (Figure 5a) and the electrostatic energy (Figure 5b) are almost negligible ( $<0.1\%$  in the total free energy) compared with others. For low monomer densities (monomer volume fractions of  $<0.1$ ), the dominant contributions to the total free energies come from the polymer–solvent interaction energy and the solvent entropy. For the particular single-chain dilute system investigated here, these contributions account for  $>50\%$  of the total free energy. Although large, these contributions are found to be almost insensitive to  $f$ . For example, polymer–solvent interaction energy changes only by less than  $0.5k_B T$  when  $l_B/l$  is varied from 0.2 to 5.0. However,  $f^*$  changes from 1 to 0 in the same range of  $l_B/l$ . In fact, the  $f$  dependent terms that significantly contribute to the total free energy are the ion-pair energy and the free ions translational entropy. At lower electrostatic interaction strengths (i.e., low  $l_B/l$ ), the translational entropy of the free ions dominates, and at higher electrostatic strengths, the ion-pair energy term significantly contributes to the free energy. Together, these two contributions account for as high as 99% of the  $f$  dependent part in the total free energy (cf. Figures 3, 4a, and 4d). Relatively very small contributions ( $\sim 1\%$ ) to the free energies come from the translational entropy of the adsorbed ions. We will see below, however, that the relative importance of a particular contribution

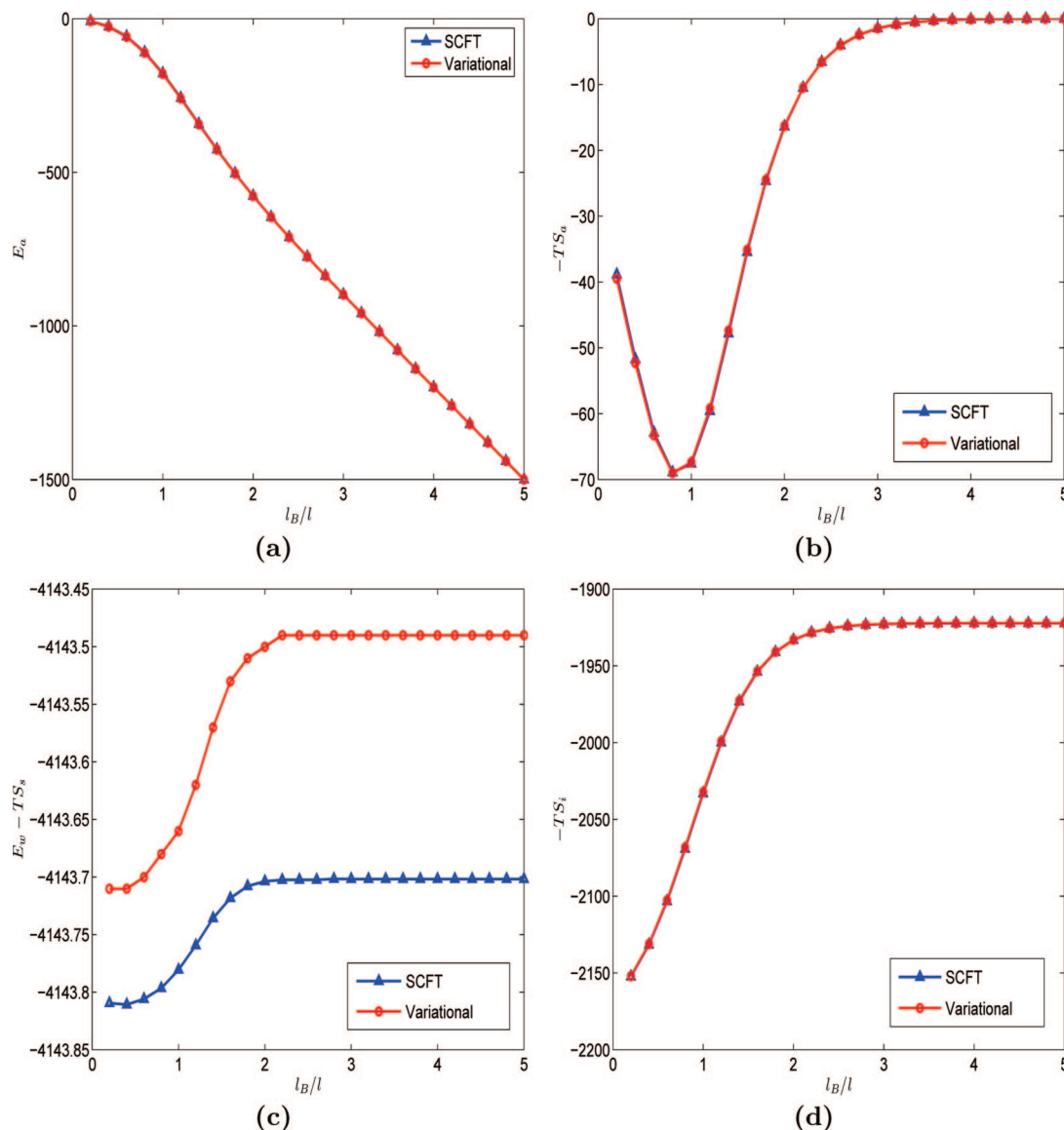
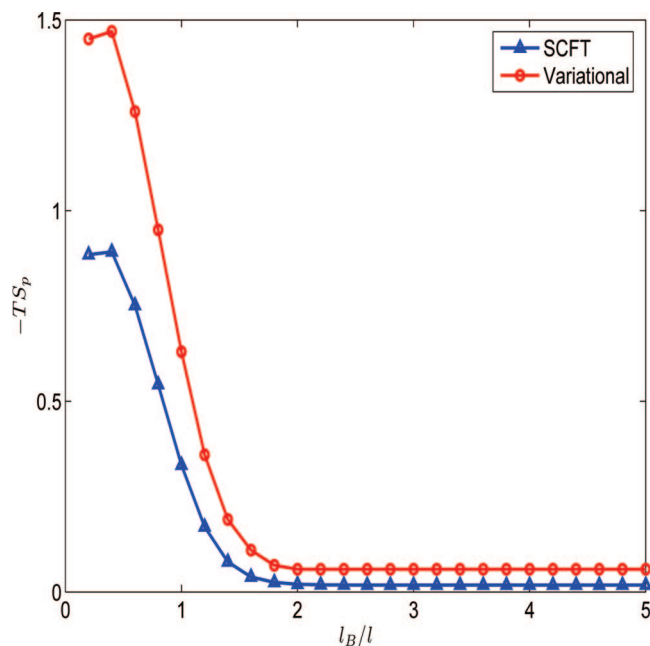


**Figure 4.** Comparison of major contributions to the free energies (presented in Figure 3) obtained from SCFT and the variational formalism. (a) Ion-pair energy contributions ( $E_a$ ), (b) translational entropy of the adsorbed counterions ( $-TS_a$ ), (c) polymer-solvent interaction energy and solvent entropy ( $E_w - TS_s$ ), and (d) translational entropy of the free ions ( $-TS_i$ ). The variational theory quantitatively captures SCFT results.

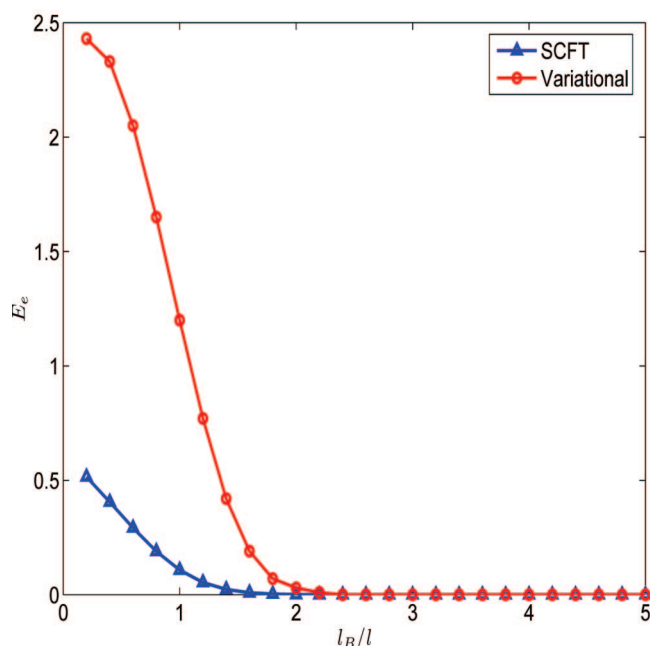
in determining the equilibrium degree of ionization is not necessarily related to its actual contribution to the total free energy.

We now discuss the various trends seen in Figures 4 and 5 on the basis of conceptual arguments aided by the different terms in Table 1. Intuitively, stronger ion-pair energy should promote counterion adsorption. As  $l_B/l$  is increased, the energy due to counterion adsorption should monotonically decrease, as seen in Figure 4a. From eq 2, it is clear that the ion-pair energy (note the negative contribution) favors counterion adsorption with a linear dependence on  $f$  and the Coulomb strength,  $l_B$ , hence a progressive gain in adsorption energy with increasing Coulomb strength (Figure 4a). However, the counterion adsorption is opposed by the translational entropy of the free ions (expression for  $TS_i$  in Table 1), hence a progressive loss of the part of the free energy related to the translational entropy (Figure 4d). The plateau in Figure 4d arises because of the completion of the adsorption of all counterions, which limits the loss in the number of free counterions (which is the number of salt ions) with increasing Coulomb strength. However, there is no plateau in Figure 4a because even after all counterions are adsorbed, the ion-pair energy continually decreases because of an increas-

ing Coulomb strength. In addition, the translational entropy of the adsorbed counterions ( $-TS_a$ ) drives the adsorption toward  $f^* = 0.5$  to optimize this part of the entropy (cf. eq 3). Physically, it can be understood from the fact that the complete adsorption of the counterions leads to the lowering of the translational entropy of the adsorbed counterions because of the unavailability of sites. Similarly, a complete desorption of the counterions also leads to the lowering of translational entropy of the adsorbed counterions because of the unavailability of the adsorbed counterions on the chain backbone. For a given  $N$ , the translational entropy of the adsorbed counterions is optimum at  $f^* = 0.5$ . We note, however, that the other two contributions might overwhelm  $-TS_a$  so that at equilibrium it is not necessarily at its minimum (Figure b). With varying Coulomb strength,  $-TS_a$  is minimum at around  $l_B/l = 0.8$ , at which  $f \approx 0.5$ , which is prevalently determined by the first two components mentioned above. The role of other contributions, that is, the polymer-solvent interaction energies and the solvent entropy (i.e.,  $E_w - TS_s$ ), the electrostatic energy involving the free ions and the monomers ( $E_e$ ), and the conformational entropy of the chain ( $-TS_p$ ) is miniscule in driving the counterion adsorption in a particular direction. However, these three contributions



(a)



(b)

**Figure 5.** Comparison of minor contributions to the free energies (presented in Figure 3). (a) Conformational entropy of the chain ( $-TS_p$ ) and (b) electrostatic energy ( $E_e$ ).

dictate the effective size of the chain (through  $l_1$ ) at equilibrium. (Note the dependence of these terms on  $l_1$  in Table 1.) Furthermore, the equilibrium counterion distribution specified by the first three contributions stipulates the actual contributions of the last three parts of the free energy at equilibrium. We previously noticed that with increasing Coulomb strength ( $l_B/l$ ) the number of free counterions (and, therefore, the effective charge of the chain) decreases. Because of a decreasing electrostatic repulsion between the monomers, the polymer chain progressively contracts until it reaches its Gaussian size at zero effective charge. Consequently, there is less mixing between the polymer and the solvent at higher Coulomb strengths, which leads to a gradual loss of polymer–solvent interaction energy (Figure 4c), which saturates to a plateau when all counterions

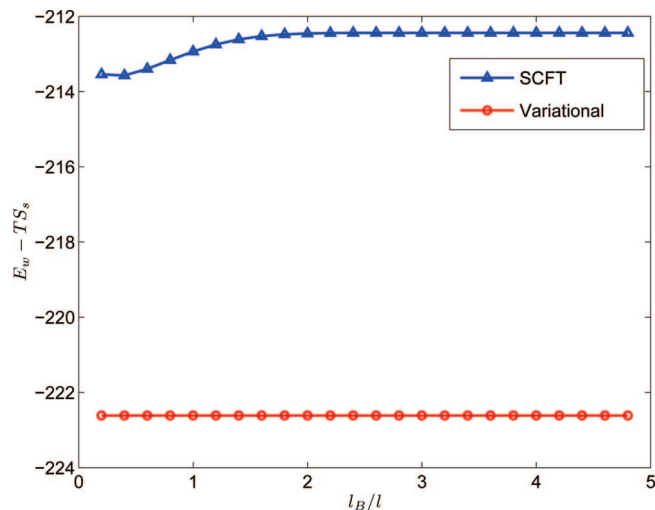


**Figure 6.** Discrepancy between SCFT and variational theory for the polymer–solvent interaction energy and solvent entropy contributions arises at high monomer densities.  $Z_p = -Z_c = -1$ ,  $R/l = 4$ ,  $N = 100$ ,  $c_s = 0.1M$ ,  $\chi_{ps} = 0.45$ , and  $\delta = 3$ .

adsorb, the physical condition that creates plateaus in all of these curves. Also accompanying the decreasing size of the chain is a gain in conformational entropy (which is maximum at the Gaussian size) observed in Figure 5a. In addition, a gradual decrease in the effective charge of the chain progressively reduces the electrostatic energy penalty observed in Figure 5b. However, this effect is very small compared with the lowering of electrostatic energy due to the formation of ion pairs, as mentioned earlier.

The quantitative agreement between the first three contributions to the free energy in two formalisms explains the observed agreement in the results obtained for  $f^*$  (Figure 2). Despite  $E_e$  having a negligible contribution to the total free energy ( $<0.1\%$ ), the comparison reveals that the Debye–Hückel estimate for the electrostatic energy ( $E_e$ ) used in the variational formalism is an overestimation (as large as five times the full, nonlinear Poisson–Boltzmann at low  $l_B/l$ ). In other words, the Debye–Hückel approximation underestimates the degree of screening, which is in agreement with other theoretical<sup>21</sup> and simulation results.<sup>37</sup> Note that the electrostatic energy in Figure 5b includes all of the charged species in the system except for the ion pairs formed on the chain by the adsorbing counterions. Nevertheless, contributions due to the electrostatic energy to total free energy are almost negligible and hence do not significantly affect  $f^*$ .

We have also carried out the same comparison of the two formalisms at higher monomer densities (above monomer volume fractions of 0.1). It is found that the discrepancy in the polymer–solvent interaction energy and the solvent entropy between the two schemes is significant. (See Figure 6.) All other contributing factors are essentially the same between the two theories. The origin of this discrepancy lies in the expansion of the  $(1 - \rho_p)\log(1 - \rho_p)$  term, which is carried up to only terms that are quadratic in polymer density in the variational calculations (Appendix B). The higher order terms in the expansion are ignored in the variational calculations to carry out the analysis analytically, which limits the applicability of the variational theory to sufficiently low monomer concentrations. The discrepancy clearly highlights the breakdown of the variational procedure at high densities and questions the use of an effective excluded volume parameter in variational calculations. However, we have not made an attempt to compute the boundary of the disagreement between the theories because our main focus of this article is on  $f$ , which is insensitive to this discrepancy. Also, the variational formalism predicts the



polymer–solvent interaction energy and the solvent entropy to be completely independent of the electrostatic interaction strength,  $l_b/l$ , in the high-density regime, which is in contrast with SCFT predictions of a weak dependence on  $l_b/l$ . (See Figure 6.) This is a result of the constraint  $R_g \leq R$ , which is used in variational calculations for mimicking the confinement effects and shows the inability of the constraint to capture the confinement effects in an appropriate fashion. Whereas the radius of gyration,  $R_g$ , of the chain readily follows from  $l_l$  in the variational formalism, it is nontrivial to compute this quantity in SCFT. In view of this, we have not addressed  $R_g$  in the present Article.

Finally, we remark on the experimental relevance of the radius parameter,  $R$ , for the confining cavity. The variational calculation readily gives  $R_g$  without any confinement for fixed values of monomer density and other parameters such as  $l_b$ ,  $\chi_{ps}$ , and  $c_s$ . Knowing this result, we have investigated the role played by the cavity radius,  $R$ , in the above analysis. If  $R$  is larger than  $R_g$ , then the above conclusions are relevant to unconfined dilute polyelectrolyte solutions. However, if  $R$  is less than  $R_g$ , then the confinement effect is manifest and our results are relevant to a polyelectrolyte chain inside a spherical pore. As an example, for  $N = 100$ ,  $c_s = 0.1M$ ,  $\chi_{ps} = 0.45$ , and  $\delta = 3$ , the calculated value of  $R_g/l$  from the variational procedure depends on  $l_b$  and attains a maximum value of 7.29, whereas  $R/l = 10.0$  in Figures 3–5. Therefore, the conclusions drawn above on the basis of these Figures are generally valid for dilute polyelectrolyte solutions. On the other hand,  $R/l = 4.0$  in Figure 6, whereas the maximum value of  $R_g$  would have been 5.92 if confinement were to be absent. Under these conditions, the conclusions regarding the discrepancy between SCFT and variational theory are pertinent to a polyelectrolyte chain confined inside a spherical cavity.

#### IV. Conclusions

In summary, we have computed the effective charge of a single flexible polyelectrolyte chain using SCFT and have compared it with the results obtained from a variational theory. It is found that for all sets of parameters, the effective degree of ionization ( $f^*$ ) computed from SCFT and the variational theory is in quantitative agreement if one-loop fluctuation corrections are deliberately suppressed in the latter. The origin of this agreement lies in the fact that  $f^*$  is determined as an interplay of the ion-pair energy and the translational entropy of the adsorbed counterions as well as of all free ions. The conformational entropy of the chain, the electrostatic energy involving the free ions and the chain, the polymer–solvent interaction energy, and the solvent entropy do not play significant roles in affecting  $f^*$ .

The comparison of different components in free energy reveals that the Debye–Hückel approximation underestimates screening effects as compared with the Poisson–Boltzmann theory. Despite the fact that there are small discrepancies in the different contributing factors to the total free energy, the effective degree of ionization ( $f^*$ ) comes out to be the same in SCFT and the truncated variational theory. Furthermore, the density fluctuations of the free ions, which are included in the full variational theory, are predicted to increase the equilibrium degree of ionization. Because this latter effect is not captured by SCFT calculations within the saddle-point approximation and because of the close agreement between SCFT and the variational theory for all other contributing factors, the variational theory appears to be a very useful tool for a quick, easy, and transparent estimation of  $f^*$ .

#### Appendix A: Self-Consistent Field Theory for Permuted Charge Distribution

Here we present a brief description of SCFT for a single flexible polyelectrolyte chain having a fixed degree of ionization ( $= f$ ) in the presence of salt ions and solvent molecules. We start from the Edward's Hamiltonian, written as

$$\exp\left(-\frac{F-F_0}{k_B T}\right) = \frac{\exp[-E_a/k_B T]}{\mu \prod_j n_j!} \int D[R] \int \prod_j \prod_{m=1}^{n_j} dr_m \times \left[ \exp\left\{-\frac{3}{2l} \int_0^N dt \left(\frac{\partial R(t)}{\partial t}\right)^2 - \chi_{ps} b^3 \int dr \hat{\rho}_p(r) \hat{\rho}_s(r) - \frac{1}{2} \int dr \int dr' \frac{\hat{\rho}_c(r) \hat{\rho}_c(r')}{4\pi\epsilon_0 \epsilon k_B T |r-r'|} \right\} \prod_r \delta(\hat{\rho}_p(r) + \hat{\rho}_s(r) - \rho_0) \delta\left(\frac{1}{l} \int_0^N dt y(t) - fNe\right) \right] \quad (A-1)$$

where  $R(t)$  represents the position vector for the  $t$ th segment and subscripts  $j = s, c, +, -$ . In eq A-1,  $k_B T$  is the Boltzmann constant times absolute temperature. In writing the interaction energies between the polyelectrolyte segments and small ions, we have taken the small ions to be point charges so that they have zero excluded volume; therefore, interactions are purely electrostatic in nature. As we consider the permuted charge distribution, the partition function has an additional sum over all possible locations of the adsorbed ions on the backbone, which appears as an average over the parameter  $y$  in eq A-1. We define the average over  $y$  as  $[\dots]_y = \int dy [\dots] g(y)$ , where  $g(y) = f\delta(y(t) - 1) + (1-f)\delta(y(t))$ .

In the above equation, the microscopic densities are defined as

$$\hat{\rho}_p(r) = \frac{1}{l} \int_0^N dt \delta(r - R(t)) \quad (A-2)$$

$$\hat{\rho}_f(r) = \sum_{i=1}^{n_j} \delta(r - r_i) \text{ for } j = s, c, +, - \quad (A-3)$$

$$\hat{\rho}_c(r) = e \left[ \frac{1}{l} \int_0^N dt Z_p y(t) \delta(r - R(t)) + \sum_{j=c,+, -} Z_j \hat{\rho}_f(r) \right] \quad (A-4)$$

where  $\hat{\rho}_p(r)$ ,  $\hat{\rho}_s(r)$ , and  $\hat{\rho}_c(r)$  stand for the monomers, small molecules (both ions and solvent molecules), and the local charge density, respectively. The Dirac delta functions involving microscopic densities enforce the incompressibility condition at all points in the system ( $\rho_0$  being the total number density of the system). The delta function involving  $y$  is a constraint that for all of the charge distributions to be considered for one particular value of  $f$ , the net charge on the chain must be a constant ( $= fNe$ ). Taking different charge distributions of the chain for the same net charge ( $= fNe$ ) and a particular chain conformation to be degenerate, the partition function is divided by the number of ways ( $\mu$ ) in which the adsorbed counterions can be distributed along the chain. If  $M$  out of total  $N$  sites on the backbone are occupied at any particular instance, then  $\mu$  is given by  $\mu = N!/(M!(N-M)!)$  so that  $1-f = M/N$ .

The dimensionless Flory parameter for chemical mismatch,  $\chi_{ps}$ , is given by  $\chi_{ps} l^3 = w_{ps} - (w_{pp} + w_{ss})/2$ , where  $w_{pp}$ ,  $w_{ss}$ , and  $w_{ps}$  are the excluded volume parameters, which characterize the short-range excluded volume interactions of type monomer–monomer, solvent–solvent, and monomer–solvent, respectively.  $F_0$  and  $E_a$  are the self-energy and ion-pair energy contributions, respectively, given by

$$\frac{F_0}{k_B T} = N w_{pp} + n_s w_{ss} \quad (A-5)$$

$$\frac{E_a}{k_B T} = -(1-f)N \delta l_b / l \quad (A-6)$$

where  $\delta = \epsilon_l / \epsilon_1 d$ , with  $\epsilon_1$  and  $d$  being the local dielectric constant and the dipole length, respectively, is used to characterize the



formation of an ion pair on the backbone because of an adsorbed counterion.

Now, using the methods of collective variables and the Hubbard–Stratonovich transformation<sup>30,31</sup> for the electrostatic part in eq A-1, the partition function can be written as integrals over the collective densities and corresponding fields so that eq A-1 becomes

$$\exp\left(-\frac{F-F_0}{k_B T}\right) = \int D[w_p]D[\rho_p]D[\psi]D[\eta] du D[w_s]D[\rho_s] \times \left[\exp\left\{-\frac{H_{scf}}{k_B T}\right\}\right]_y \quad (\text{A-7})$$

Here  $w_p$  and  $w_s$  are the fields experienced by the monomers and solvent, respectively, and  $\rho_p$  and  $\rho_s$  represent their respective collective densities. All charged species (excluding the ion pairs formed because of adsorption of counterions) experience a field,  $\psi$  (which is equivalent to the electrostatic potential).  $\eta$  and  $u$  are Lagrange's multipliers corresponding to, respectively, the incompressibility and net charge constraints in the partition function. We must stress here that this procedure is equivalent to introducing collective fields and densities for small ions instead of using the Hubbard–Stratonovich transformation for the electrostatics part.

Within SCFT, the functional integrals over the fields and the densities are approximated by the value of the integrand at the extremum (also known as the saddle-point approximation). Extremizing the integrand leads to a number of nonlinear equations for the fields and the densities. The saddle point approximation with respect to  $u$  gives equations similar to a smeared charge distribution, where every monomer has a charge ( $= fe$ ). The extremization with respect to  $\psi$ ,  $w_p$ ,  $\rho_p$ ,  $\eta$ ,  $w_s$ , and  $\rho_s$  leads to the saddle point specified by eqs 4–6 and 8–11. By using these saddle point equations and employing the Stirling's approximation for  $\ln n!$ , we obtain the approximated free energy, that is,  $F - F_0 \approx H_{scf}^*$ , as presented in section IIA after taking  $k_B T = 1$ . The superscript \* represents the saddle point estimate of the free energy.

## Appendix B: Variational Theory

In this appendix, we present the procedure for obtaining the variational free energy as presented in ref 26 in the absence of ion-pair correlations. In ref 26, it has been assumed that the counterions from the polyelectrolyte are indistinguishable from the counterions from the salt. Therefore, we start from a partition function similar to eq A-1 with the solvent, counterions (from the polyelectrolyte and the salt), coions, and the chain as distinguishable species. After the use of collective variables, the partition function can be written as

$$\exp\left(-\frac{F-F_0}{k_B T}\right) = \int D[w_p]D[\rho_p]D[\eta] \prod_j D[\rho_j]D[w_j] \times \exp\left\{-\frac{h}{k_B T}\right\} \quad (\text{B-1})$$

where  $j = s, c, -$  and where the integral over  $u$  has already been evaluated by the saddle point method so that the functional  $h$  corresponds to a single chain with a smeared charge distribution. Here we have introduced collective fields and densities for small ions instead of using the Hubbard–Stratonovich transformation for the electrostatic part (as already pointed out in Appendix A). This is the analog of eq A-7 in SCFT. Now, evaluating the path integrals over  $w_j$  by the saddle point method, eq B-1 can be written in terms of the densities,  $\rho_j$ . Functional integrals over  $\eta$  and  $\rho_s$  can be carried out in a trivial way. To carry out functional integrals over small ion densities, the  $\rho_j \log \rho_j$  terms, which emerge after integrations over fields,  $w_j$ , are expanded up to the quadratic terms after writing  $\rho_j(r) = n_j/\Omega + \delta\rho_j(r)$  so that  $dr \delta\rho_j(r) = 0$  and the resulting integrals are Gaussian. This procedure also gives one-loop corrections to the free energy coming from the small ions density fluctuations

$(\Delta F/k_B T)$ . Now, expanding the  $(1 - \rho_p) \log(1 - \rho_p)$  term up to the quadratic terms in  $\rho_p$ , the problem of carrying out the functional integrals over  $w_p$  and  $\rho_p$  is equivalent to a single-chain problem whose monomers interact with each other via a renormalized excluded volume parameter and an electrostatic potential. The renormalized excluded volume parameter comes out to be  $w = 1 - 2\chi_{ps}$ , and the electrostatic potential comes out to be the Debye–Hückel potential, where the inverse Debye length ( $\kappa$ ) depends on only the free ions. Eventually, eq B-1 becomes

$$\exp\left(-\frac{F-F_0-\delta F}{k_B T}\right) = \frac{1}{\mu} \exp\left\{-\frac{E_a - TS_i}{k_B T}\right\} \int D[w_p]D[\rho_p] \times \exp\left\{-\frac{H_{var}}{k_B T}\right\} \quad (\text{B-2})$$

where  $-TS_i$  is the translational entropy of the free ions, as presented in Table 1 for the variational theory. Now, writing the Hamiltonian of a single polyelectrolyte chain using an effective excluded parameter ( $w$ ) and the Debye–Hückel potential,<sup>26</sup> the functional integrals over  $w_p$  and  $\rho_p$  can be computed using the variational technique developed by Muthukumar.<sup>33</sup> Taking  $k_B T = 1$ , the results are presented in section IIB.

**Acknowledgment.** We acknowledge financial support from the National Institutes of Health (grant no. R01HG002776), National Science Foundation (grant no. DMR-0605833), AFOSR (FA9550-07-1-0347), and the Material Research Science and Engineering Center at the University of Massachusetts, Amherst.

## References and Notes

- (1) Rice, S. A.; Nagasawa, M. *Polyelectrolyte Solutions: A Theoretical Introduction*; Academic Press: London, 1961.
- (2) Manning, G. S. *J. Chem. Phys.* **1969**, *51*, 924–933.
- (3) Dautzenberg, H.; Jaeger, W.; Kotz, J. *Polyelectrolytes: Formation, Characterization, and Application*; Hanser Publishers: New York, 1994.
- (4) Volk, N.; Vollmer, D.; Schmidt, M.; Oppermann, W.; Huber, K. *Adv. Polym. Sci.* **2004**, *166*, 29–65.
- (5) Stevens, M. J.; Kremer, K. *J. Chem. Phys.* **1995**, *103*, 1669–1690.
- (6) Winkler, R. G.; Gold, M.; Reineker, P. *Phys. Rev. Lett.* **1998**, *80*, 3731–3734.
- (7) Liu, S.; Muthukumar, M. *J. Chem. Phys.* **2002**, *116*, 9975–9982.
- (8) Liu, S.; Ghosh, K.; Muthukumar, M. *J. Chem. Phys.* **2003**, *119*, 1813–1823.
- (9) Liao, Q.; Dobrynin, A. V.; Rubinstein, M. *Macromolecules* **2003**, *36*, 3399–3410.
- (10) Liao, Q.; Dobrynin, A. V.; Rubinstein, M. *Macromolecules* **2006**, *39*, 1920–1938.
- (11) Hsiao, P. Y.; Luijten, E. *Phys. Rev. Lett.* **2006**, *97*, 148301.
- (12) Chang, R. W.; Yethiraj, A. *Macromolecules* **2006**, *39*, 821–828.
- (13) Beer, M.; Schmidt, M.; Muthukumar, M. *Macromolecules* **1997**, *30*, 8375–8385.
- (14) Bordini, F.; Cametti, C.; Tan, J. S.; Boris, D. C.; Krause, W. E.; Plucktaevesak, N.; Colby, R. H. *Macromolecules* **2002**, *35*, 7031–7038.
- (15) Schweins, R.; Hollmann, J.; Huber, K. *Polymer* **2003**, *44*, 7131–7141.
- (16) Prabhu, V. M.; Amis, E. J.; Bossev, D. P.; Rosov, N. *J. Chem. Phys.* **2004**, *121*, 4424–4429.
- (17) Popov, A.; Hoagland, D. A. *J. Polym. Sci., Part B: Polym. Phys.* **2004**, *42*, 3616–3627.
- (18) Essafi, W.; Lafuma, F.; Baigl, D.; Williams, C. E. *Europhys. Lett.* **2005**, *71*, 938–944.
- (19) Prabhu, V. M. *Curr. Opin. Colloid Interface Sci.* **2005**, *10*, 2–8.
- (20) González-Mozuelos, P.; Olvera de la Cruz, M. *J. Chem. Phys.* **1995**, *103*, 3145–3157.
- (21) Stigter, D. *Biophys. J.* **1995**, *69*, 380–388.
- (22) Brilliantov, N. V.; Kuznetsov, D. V.; Klein, R. *Phys. Rev. Lett.* **1998**, *81*, 1433–1436.
- (23) Schiessel, H.; Pincus, P. *Macromolecules* **1998**, *31*, 7953–7959.
- (24) Kuhn, P. S.; Barbosa, M. C. *Physica A* **2005**, *357*, 142–149.
- (25) Liverpool, T. B.; Muller-Nedebock, K. K. *J. Phys.: Condens. Matter* **2006**, *18*, L135–L142.
- (26) Muthukumar, M. *J. Chem. Phys.* **2004**, *120*, 9343–9350.
- (27) Grosberg, A. Y.; Nguyen, T. T.; Shklovskii, B. I. *Rev. Mod. Phys.* **2002**, *74*, 329–345.
- (28) Kundagrami, A.; Muthukumar, M. *J. Chem. Phys.* **2008**, *128*, 244901.

- (29) Borukhov, I.; Andelman, D.; Orland, H. *Eur. Phys. J. B* **1998**, 5, 869–880.
- (30) Fredrickson, G. H. *The Equilibrium Theory of Inhomogeneous Polymers*; Oxford University Press: New York, **2006**.
- (31) Kumar, R.; Muthukumar, M. *J. Chem. Phys.* **2008**, 128, 184902.
- (32) Muthukumar, M.; Edwards, S. F. *J. Chem. Phys.* **1982**, 76, 2720–2730.
- (33) Muthukumar, M. *J. Chem. Phys.* **1987**, 86, 7230–7235.
- (34) Edwards, S. F. *Proc. Phys. Soc., London* **1965**, 85, 613–624.
- (35) Muthukumar, M. *J. Chem. Phys.* **2003**, 118, 5174–5184.
- (36) Press, W. H.; Teukolsky, S. A.; Vetterling, W. T.; Flannery, B. P. *Numerical Recipes in C: The Art of Scientific Computing*; Cambridge University Press: New York, 1992.
- (37) Stevens, M. J.; Kremer, K. *J. Phys. II* **1996**, 6, 1607–1613.

MA801799E